

Experimental Evidence of Quantum Radiation Reaction in Aligned Crystals

Tobias N. Wistisen,^{1*} Antonino Di Piazza,² Helge V. Knudsen,¹ Ulrik I. Uggerhøj¹

¹Department of Physics and Astronomy, Aarhus University,
Ny Munkegade 120, Aarhus, 8000, Denmark

²Max Planck Institute for Nuclear Physics,
Saupfercheckweg 1, Heidelberg, 69117, Germany

*To whom correspondence should be addressed; E-mail: tobiasnw@phys.au.dk.

November 26, 2021

Radiation reaction is the influence of the electromagnetic field emitted by a charged particle on the dynamics of the particle itself. Taking into account radiation reaction is essential for the correct description of the motion of high-energy particles driven by strong electromagnetic fields. Classical theoretical approaches to radiation reaction lead to physical inconsistent equations of motion. A full understanding of the origin of radiation reaction and its consistent description are possible only within the more fundamental quantum electrodynamical theory. However, radiation-reaction effects have never been measured, which has prevented a complete understanding of this problem. Here we report experimental radiation emission spectra from ultrarelativistic positrons in silicon in a regime where both quantum and radiation-reaction effects dominate the dynamics of the positrons. We found that each positron emits multiple photons with energy comparable to its own energy, revealing the importance of quantum photon recoil. Moreover, the shape of the emission spectra indicates that photon emissions occur in a nonlinear regime where positrons absorb several quanta from the crystal field. Our theoretical analysis shows that only a full quantum theory of radiation reaction is capable of explaining the experimental results, with radiation-reaction effects arising from the recoils undergone by the positrons during multiple photon emissions. This experiment is the first fundamental test of quantum electrodynamics in a new regime where the dynamics of charged particles is determined not only by the external electromagnetic fields but also by the radiation-field generated by the charges themselves. Future experiments carried out in the same line will be able to, in principle, also shed light on the fundamental question about the structure of the electromagnetic field close to elementary charges.

A complete understanding of the dynamics of charged particles in external electromagnetic fields is of fundamental importance in several branches of physics, spanning e.g. from pure theoretical areas like particle physics, to more applicative ones like accelerator physics. Since accelerated charges, electrons for definiteness, emit electromagnetic radiation, in the realm of classical electrodynamics a self-consistent equation of motion of the electron in an external electromagnetic field must take into account the resulting loss of energy and momentum [32, 31]. However, the inclusion of the reaction of the radiation emitted by an electron on the motion of the electron itself (radiation reaction) leads to one of the most famous and controversial equations of classical electrodynamics, the Lorentz-Abraham-Dirac (LAD) equation [3, 4, 5, 6, 7]. The LAD equation is plagued by serious inconsistencies like the existence of “runaway” solutions, with the electron acceleration diverging exponentially in time even if the external field identically vanishes. The mentioned exponential growth is found to occur at time scales of the order of the time that light needs to cover the classical electron radius $r_e = e^2/mc^2 = 2.8 \times 10^{-15}$ m, i.e. $\tau = r_e/c = 9.5 \times 10^{-24}$ s [32, 31, 7]. Now, the classical electron radius is $\alpha = e^2/\hbar c \simeq 1/137$ times smaller than the reduced Compton wavelength $\lambda_C = \hbar/mc = 3.9 \times 10^{-13}$ m, which is the typical length of quantum electrodynamics (QED) [8] and this also applies to the time scale τ . This occurrence suggests that a complete understanding of the problem of radiation reaction requires an approach based on QED. Below we will concentrate on a regime where both quantum and radiation-reaction effects are substantial, and we therefore refer the reader to the recent reviews [9, 10, 11] concerning classical aspects of radiation reaction. We only recall here that the discussed overlapping between classical and quantum scales implies that within the realm of classical electrodynamics the LAD equation can be consistently approximated by an equation, known as Landau-Lifshitz (LL) equation, which is not plagued by the above-mentioned inconsistencies [31]. In order for quantum

effects to be negligible, in the instantaneous rest frame of a relativistic electron the external field has to vary slowly on space (time) distances of the order of λ_C (λ_C/c) and its amplitude has to be much smaller than the so-called critical electric (magnetic) field of QED $E_{cr} = m^2 c^3 / \hbar |e| = 1.3 \times 10^{18}$ V/m ($B_{cr} = m^2 c^3 / \hbar |e| = 4.4 \times 10^9$ T) [8, 12, 13, 36]. These conditions guarantee, among others, that the recoil undergone by the electron during the emission of a single photon inside the considered field, is much smaller than the electron energy and the whole emission process can be treated classically as a continuous emission. In the situation investigated below, the second mentioned condition plays a major role and, if we define the parameter $\chi = \gamma E / E_{cr}$, where E is a measure of the amplitude of the crystal electric field and where γ is the electron Lorentz factor, it can be expressed as $\chi \ll 1$. The relation between radiation reaction and the emission of multiple photons in a regime where quantum recoil is substantial has been pointed out in [39] in the interaction of ultrarelativistic electrons with intense laser fields. In the quantum radiation reaction regime the typical energy of the emitted photons is comparable to the energy of the incoming electron ($\chi \gtrsim 1$) and multiple photon emission is more probable than single photon emission. In laser-electron interaction it is customary to assume the laser field to be “strong” in the sense that the parameter $\xi_l = |e| E_l / m c \omega_l$, where E_l and ω_l are the laser amplitude and the angular frequency, respectively, is much larger than unity [38, 39, 17]. At $\xi_l \gg 1$ each photon emission occurs with the absorption of several laser photons and the radiation is formed over a length (formation length) much shorter than the laser wavelength. Thus, the formula of the radiation emission probability in a constant crossed field (CCF) can be employed [36, 18, 8]. A more general definition of the parameter ξ_l (indicated below as ξ) is related to the importance of relativistic effects in the electron transverse motion, with respect to the direction of its average velocity: $\xi = p_{\perp, \max} / m c$, where $p_{\perp} = \gamma m v_{\perp}$ is the transverse momentum [36]. In the ultrarela-

tivistic regime the parameter ξ also represents the maximum angular deflection during the electron's motion from its average direction, divided by the characteristic angle of radiation $1/\gamma$. In the terminology used in [36] the conditions $\xi \ll 1$ and $\xi \gg 1$ thus correspond to the dipole and the magnetic bremsstrahlung (or CCF) limits, respectively.

One of the main reasons why such an old, fundamental and outstanding problem as the radiation reaction problem is still unsolved, relies on the difficulties in detecting it experimentally. As we have hinted above, the rapid development of laser technology has renewed the interest in this problem because the strong fields provided by intense laser facilities may allow for the experimental measurement of radiation-reaction effects (we refer to the review [10] for papers until 2012 and we also mention the recent studies [19, 20, 17, 21, 22, 38, 23, 24, 25, 26, 27]). In [28] we have realized that the strong electric fields in aligned crystals may be also suitable for measuring radiation-reaction effects and test the LL equation. In an aligned crystal, in fact, under suitable conditions identifying the so-called channeling regime, an electric charge also oscillates similarly as in a laser field and may thus radiate a substantial fraction of its energy.

In the experiment described below, ultrarelativistic positrons cross a Si crystal in the channeling regime. The dynamics of the positrons is characterized by $\chi \leq 1.4$ and $0.7 \lesssim \xi \lesssim 7$ such that one is in the quantum regime and the field is either classically strong or in an intermediate regime below the CCF regime $\xi \gg 1$. The experiment has been performed at the SPS NA facility at CERN employing positrons with incoming energy of $\varepsilon_0 = 178.2$ GeV and two Si crystals with thickness 3.8 mm and 10 mm, respectively, aligned along the $\langle 111 \rangle$ axis. The measured photon emission spectra show features which can only be explained theoretically by including both 1) quantum effects related to the recoil undergone by the positrons in the emission of photons and the stochasticity of photon emission, and 2) radiation-reaction effects stemming from the emission of multiple

photons. Several experiments have studied the emission of radiation in crystals in the quantum regime, mostly in thin crystals to avoid pile-up effects in the calorimeter i.e. the emission of multiple photons by a single particle has been avoided. Due to pile-up, in fact, only the sum of the energies of all the photons emitted by each charged particle is measured in such experiments, which prevents the possibility of reconstructing the single-photon spectrum (in e.g. [29] such a pile-up effect can be seen). In the present experiment we have instead employed a thin converter foil and a magnetic spectrometer to obtain the single-photon spectrum, see figure 1. Therefore, in the radiation-reaction regime where many photons are emitted by a single positron, the current experiment clearly provides more information on the dynamics of the positrons and a stronger test of the theory than previous experimental campaigns.

In figure 1 a schematic of the experimental setup is shown. The incoming positron encounters the scintillators S1, S2 and S3 which are used to make the trigger signal. The positron rate is sufficiently low such that in each event only a single positron enters the setup. The positron then enters a He chamber where the two first position sensitive ($2\text{ cm} \times 1\text{ cm}$) MIMOSA-26 detectors are placed. Shortly after the He chamber the crystal target is placed. The He chamber reduces multiple scattering of the positron such that the incoming particle angle can be measured precisely using the detectors M1 and M2. After the positron enters the crystal, multiple photons and charged particles will leave the crystal. We have ensured also theoretically that electron-positron pair production by the emitted photons is negligible in the considered experimental conditions. To sweep away the charged particles, two large magnets were placed before the final set of tracking detectors. The photons emitted inside the crystal then reach a thin converter foil, $200\text{ }\mu\text{m}$ of Ta, corresponding to approximately 5% of the radiation length X_0 , which in turn corresponds to $7/9$ of the mean free path for pair production by a high-energy photon

[45]. The thickness was optimized such that most of the time a single photon among those emitted by each positron converts to an electron-positron pair. The produced pair then passes through M3 and M4 before entering a small magnet, such that the momenta of the electron and the positron can be determined based on the resulting angular deflection. Finally, the deflected electron and positron pass through M5 and M6. As we have mentioned, unlike using a calorimeter, this setup has the great advantage that it allows one to measure the single-photon radiation spectrum since only a single, randomly chosen, of the several emitted photons converts to a pair in the thin foil. It is important to point out that for photon energies much larger than the electron rest energy, as most of those emitted in our experiment, the conversion of a photon into an electron-positron pair in the thin foil is independent of the photon energy [45]. Thus, the presence of the thin foil does not alter the spectrum of the photons emitted in the crystal. The tracking algorithm used in the analysis of the data to correctly determine the energy of the photon which originated from the measured electron and positron is described in the Supplementary Materials. It is clear that the spectrum originating from this procedure can not be directly compared to the theory since the response of the setup is complicated by “practical” effects such as multiple scattering in the converter foil and the presence of air. Therefore a simulation of the experimental setup which can “translate” the theoretical photon spectra into the corresponding experimental ones has been developed, the details of which can also be found in the Supplementary Materials.

In figure 2, left panel, we show the experimentally obtained counting spectra for the “background” case, when no crystal is present, for the “random” case when the crystal is present but not aligned with respect to the positron beam, and for the “align” case, when the crystal’s $\langle 111 \rangle$ axis is aligned with the positron beam. In the right panel we show a comparison of the experimental and the theoretical results in the amorphous case.

The theoretical, simulated curves, are denoted by “sim” (see also the Supplementary Materials). In the vertical label of this plot $X_0 = 9.37$ cm is the radiation length of Si. In the random orientation the radiation emission is the well understood Bethe-Heitler bremsstrahlung [45] and the agreement here therefore shows that the simulation of the setup is accurate. The result in the random orientation was used as a way to normalize the theoretical results to the experiment by a scaling factor. This is necessary since the efficiency of the setup depends not only on the geometry of the setup, multiple scattering etc., but also on the inherent efficiency of the MIMOSA detectors.

We have considered four different theoretical models to compare with the experiment. These models are described in the section Materials and Methods in the Supplementary Materials, and, depending on which effects they include, are indicated as classical plus radiation reaction model (CRRM), semiclassical plus radiation reaction model (SCRRM), quantum plus radiation reaction model (QRRM), and quantum with no radiation reaction model (QnoRRM). In figure 3 we show the result of such a comparison in the cases of the 3.8mm crystal (left) and the 10.0mm crystal (right). As we have anticipated, among the four models described in the Supplementary materials, only the QRRM can be considered in reasonable agreement with the experimental data, indicating the importance of including both quantum and radiation-reaction effects in the modeling. As we have also hinted, the remaining discrepancy can likely be attributed to the use of the CCF approximation in regions at the limits of its applicability. However, to the best of our knowledge, no complete theory of quantum radiation reaction, valid in all regimes, has yet been devised as it would essentially imply an exact computation of the emission probability of an arbitrary number of hard photons.

For the sake of completeness, in figure 4 we show the positron power spectra according to the four mentioned theoretical models before the translation based on the simulation

of the setup has been carried out. Here it is seen that for both thicknesses the curves corresponding to the “QnoRRM” are the same but that this is not the case after the translation is carried out (see figure 3). The main reason for this is that the efficiency of the experimental setup depends on the total number of produced photons. This effect becomes severe when the number of photons that can convert in the foil becomes appreciable compared to ~ 26 , considering the 5% of the radiation length X_0 converter foil such that multi-photon conversion becomes likely. In such events the original photon energy can not be found and is thus rejected (this also shows the necessity of doing such a simulation of the experimental setup). It is seen in the 3.8 mm case that there is a qualitative agreement between figure 3 and figure 4 in the relative sizes of the spectra compared to each other. However, in the case of the 10.0 mm crystal it is seen, for example, that the spectrum corresponding to the “QRRM” model is higher than that corresponding to the “SCRRM” in figure 3, whereas the opposite occurs in figure 4. This is possible due to the many more soft photons being predicted in the “SCRRM” calculation than in the “QRRM”, which lowers the translated spectrum because of the discussed rejection of multi photon conversion events in the foil.

Supplementary Materials and Methods

Theoretical Models We have considered four different theoretical models to compare with the experiment:

1. Classical plus radiation reaction model (CRRM). In this model, we include radiation reaction classically, i.e., we determine the positron trajectory via the Landau-Lifshitz (LL) equation $mcdu^i/ds = (q/c)F^{ij}u_j + g^i$, where (see, e.g., [31])

$$g^i = \frac{2q^3}{3mc^3} \frac{\partial F^{ik}}{\partial x^l} u_k u^l - \frac{2q^4}{3m^2 c^5} F^{il} F_{kl} u^k + \frac{2q^4}{3m^2 c^5} (F_{kl} u^l) (F^{km} u_m) u^i. \quad (1)$$

Top View

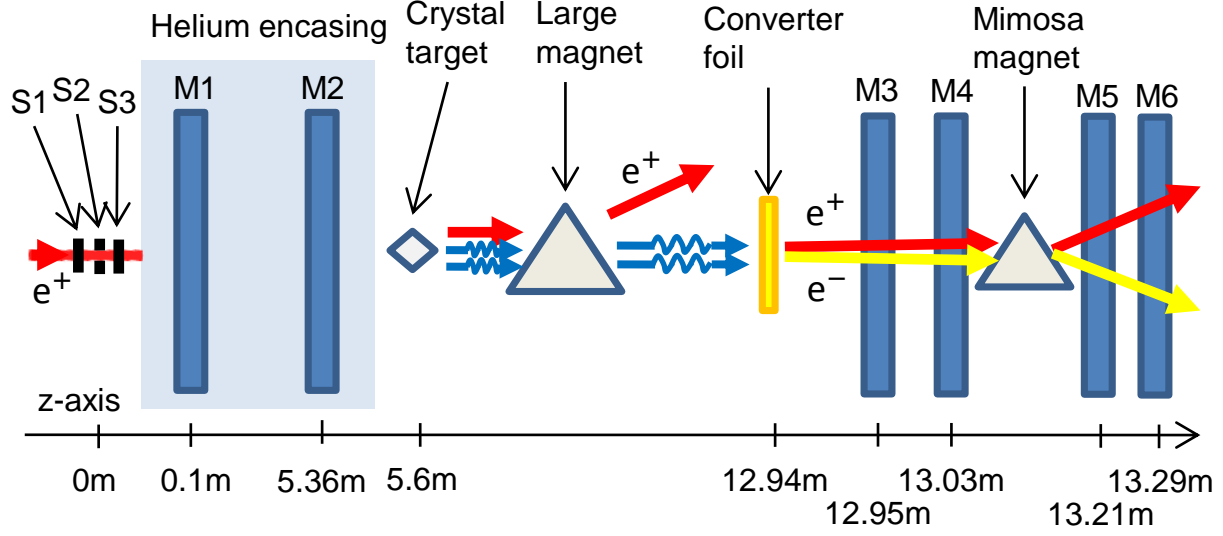


Figure 1: Experimental setup. A schematic representation of the experimental setup in the H4 beam line in the SPS North Area at CERN. The symbols “Sj”, with $j = 1, 2, 3$ denote the scintillators and the symbols “Mi”, with $i = 1, \dots, 6$, denote MIMOSA position sensitive detectors.

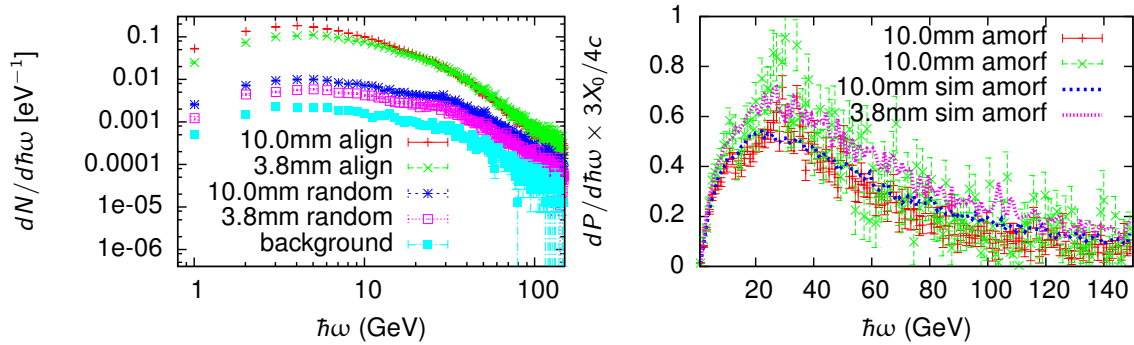


Figure 2: Experimental counting spectra and comparison to simulation in random orientation. Photon counting spectra per single incoming positron for the two crystal thicknesses indicated in the text in the aligned and the random case along with a measurement of the background radiation (left panel). The background subtracted power spectrum in the random orientation are compared to simulations (right panel).

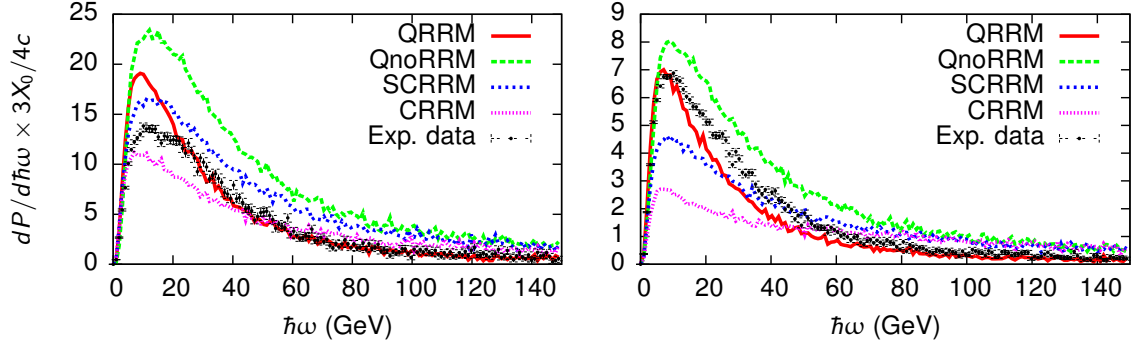


Figure 3: Experimental power spectra. Background subtracted power spectra in the aligned case for two crystal thicknesses: 3.8 mm (left panel) and 10.0 mm (right panel). The experimental data are compared to the four different theoretical models described in the Supplementary Materials after being translated through the simulation of the experimental setup.

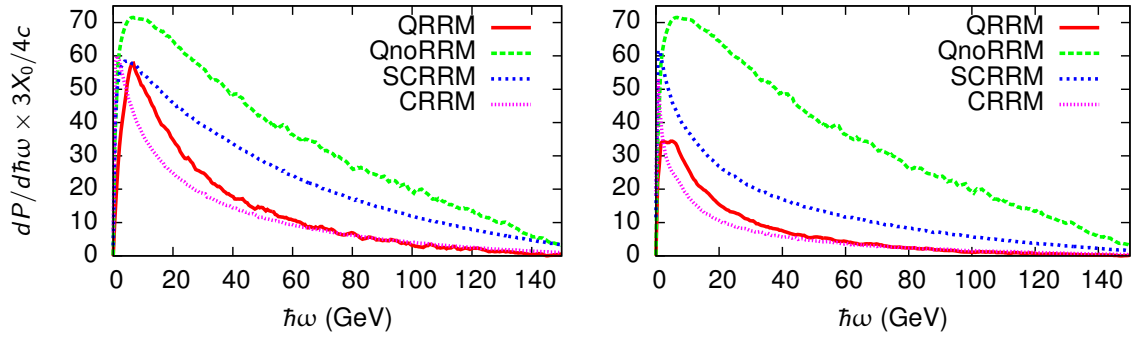


Figure 4: Theoretical power spectra. Power spectra calculated according to the four different theoretical models described in the Supplementary Materials for the two crystal thicknesses: 3.8 mm (left panel) and 10.0 mm (right panel).

Here, u^i is the positron four-velocity, s its proper-time, $q = e > 0$ and m its charge and mass respectively, and F^{ij} the electromagnetic field tensor of the crystal (see, e.g., [32]). The crystal field has been modeled starting from the sum of Doyle-Turner string potentials [33], centered on a regular grid according to the diamond cubic crystal structure. Once the positron trajectory has been determined, the emission spectrum has been computed starting from the Liénard-Wiechert potential and following the standard procedure, as described, e.g., in [32].

2. Semiclassical plus radiation reaction model (SCRRM). In this model we “partially” include quantum effects following an approach described, e.g., in [34], where the term involving the derivative in Eq. (1) is neglected and the remaining two are multiplied by the ratio between the quantum total emitted power and the corresponding classical quantity. The emission spectrum has then been evaluated as in the CRRM. This model phenomenologically takes into account that quantum effects reduce the total radiation yield but it does not account for the intrinsic stochasticity of the photon emission process (see, e.g., [35]).
3. Quantum plus radiation reaction model (QRRM). In this model the radiation emission is taken into account fully quantum mechanically, i.e., the positron propagates classically within the crystal according to the Lorentz equation and, in a genuinely random way, it emits photons and undergoes the corresponding recoil. A numerical program has been written to determine the positron dynamics and emission spectrum according to the following procedure. At each step in the time evolution of the positron trajectory the probability of single photon emission in that time interval is originally calculated within the constant-crossed field (CCF) approximation (see, e.g., Eq. (4.36) in [36]) and a random number generator decides if the emission takes

place or not (the time step has been chosen sufficiently small such that the resulting single-photon emission probability is much smaller than unity). In the former case, on the one hand, the photon energy is also determined by sampling another random number using the procedure shown in [37], such that the emitted photons are consistently distributed in accordance with the formula for radiation emission also in the CCF approximation (see Eq. (4.24) in [36]). On the other hand, the momentum of the emitted photon is directed along the positron momentum at the instant of emission (which is an excellent approximation in the ultrarelativistic regime) and it is subtracted from the positron momentum before the trajectory solver starts out with the new initial conditions according to the Lorentz equation. As we have mentioned, the emission probabilities within the CCF approximation are employed here (like in e.g. [35, 38, 39]). However, since ξ is in some cases only comparable to unity in the experiment, the model has been improved. In fact, for low energies of the emitted photons $\hbar\omega \ll \varepsilon_0$, the formation length of the emission process is given by $l_f(\omega) = 2\gamma^2 c/\omega$, where γ is the Lorentz factor of the positron at the instant of emission [36]. Thus, if we denote as λ_0 the typical oscillation length of a channeled positron, we expect that the CCF approximation does not work for frequencies lower than ω_c , with $l_f(\omega_c) = a\lambda_0/2$, where a is a constant of the order of unity. In order to determine the constant a , we have used the fact that at low photon energies, where it is not valid, the CCF approximation significantly overestimates the emitted radiation yield with respect to the more general and more accurate approach of Baier et. al. described in [36, 40, 41, 42] and also used numerically in several channeling codes [43, 44]. Thus, as the simplest approach, we have modified the CCF emission probability by setting it to zero for photon frequencies below ω_c . The constant a has been fixed by requiring that the resulting total yield coincides with the total yield

given by the more accurate approach by Baier et al. [36, 40, 41, 42] in the case of a thin crystal where multiple photon emissions are negligible. Indeed, we have found numerically that in this way a turns out to be approximately equal to 0.52.

4. Quantum with no radiation reaction model (QnoRRM). This model is the same as the QRRM described above but whenever the positron emits a photon, its recoil energy-momentum is not subtracted from the positron. The spectrum in the QRRM approaches the spectrum of this model when the crystal becomes thin because for a thin crystal the probability of multiple photon emission becomes negligible and each positron essentially emits a single photon. Thus, the difference between this model and the QRRM shows the size of the effects of the recoil of multiple photon emission, i.e. of radiation reaction.

Tracking Algorithm A tracking algorithm has been employed in the analysis of the experimental data in order to correctly characterize the created electrons and positrons, and determine whether they arise from a converting photon in the foil. This is decided based on a series of conditions: Hypothetical rectilinear tracks in the detectors M3-M4 and M5-M6 (see figure 1 in the main text) are constructed by connecting all possible pairs of hits in the two planes of M3-M4 and in the two planes of M5-M6. These track candidates in M5-M6 must be matched with those in M3-M4 giving a full particle track, identified by the following conditions:

1. The tracks for individual particles arising from two points in M3-M4 and from two points in M5-M6 are ideally continued into the magnet and, in order to be accepted, they must have a distance to each other within 0.8 mm in the center of the magnet.
2. The two tracks from the detectors M3-M4 and M5-M6 should be at the shortest distance from each other approximately at the z position of the center of the magnet.

3. The size of the deflection angle between the tracks in M5-M6 and the tracks in M3-M4 in the y direction must be smaller than 2 mrad because the magnet deflects only along the x direction.

Now, tracks of electrons and positrons have been individually identified. Moreover, these must also be paired to stem from the same photon. This identification is carried out by requiring that an electron and a positron track must originate from within a distance of 20 μm on the x - y plane in the converter foil. After the identification of the tracks has been carried out, it may happen that for a given electron or positron, more than one particle of opposite charge matches within the mentioned distance in the converter foil. If this happens, the event is discarded because more than one photon must have converted in the foil and it is not possible to unequivocally associate the electron-positron pair with a photon.

This also implies that if the number of photons above the pair production threshold in the converter foil exceeds ~ 26 , one will begin to see the experimental photon spectrum drop due to multiple photon conversion. We recall that, as we have mentioned in the main text, the thickness of the converter foil corresponds to about $(7/9) \times 5\% \simeq 1/26$ of the average length that a photon covers before converting into an electron positron pair. Therefore, optimally, this regime is avoided.

In each event all tracks are determined in M1, M2, and M3 as well. The chosen track in these detectors is the one with the closest approach to the pair origin already determined in the converter foil. Finally, the positron entry angle is determined from the hits in M1 and M2 of this track.

It is clear that the photon energy spectrum originating from this procedure can not be directly compared to the theoretical spectra because the response of this setup is complicated by practical issues. For example, a positron entering the setup at the center of

the detector M1 and another one entering at the border of the same detector will have a different chance of leading to a detected pair. The reason is that the pair originating from the positron hitting M1 at the border is more likely to be deflected outside M5 or M6. A similar effect takes place when considering the angle of the incoming positrons. In addition to this, multiple scattering in the converter foil, air and detectors influence both the efficiency and the resolution. In order to deal with these issues, a code simulating the setup has been written. The beam distribution in position and angle as experimentally measured are given as input to the program simulating the setup, and then the effects of multiple Coulomb scattering between and inside the detectors and converter foil, as well as of the Bethe-Heitler pair-production are included for determining the particles' dynamics [45]. The only non-trivial input to such a simulation of the setup, is the spectrum of the radiation emitted by the positrons in the crystal, which we have determined theoretically according to the four models described above. Finally, the simulation of the setup produces data-files of the same format as those obtained from the data acquisition in the experiment, which are then both sent through the tracking algorithm.

References and Notes

- [1] J. D. Jackson, *Classical Electrodynamics* (Wiley, New York, 1975).
- [2] L. D. Landau, E. M. Lifshitz, *The Classical Theory of Fields* (Elsevier, Oxford, 1975).
- [3] M. Abraham, *Theorie der Elektrizität* (Teubner, Leipzig, 1905).
- [4] H. A. Lorentz, *The Theory of Electrons* (Teubner, Leipzig, 1909).
- [5] P. A. M. Dirac, *Proc. R. Soc. London, Ser. A* **167**, 148 (1938).

- [6] A. O. Barut, *Electrodynamics and Classical Theory of Fields and Particles* (Dover Publications, New York, 1980).
- [7] F. Rohrlich, *Classical Charged Particles* (World Scientific, Singapore, 2007).
- [8] V. B. Berestetskii, E. M. Lifshitz, L. P. Pitaevskii, *Quantum Electrodynamics* (Elsevier Butterworth-Heinemann, Oxford, 1982).
- [9] R. T. Hammond, *Electron. J. Theor. Phys.* **7**, 221 (2010).
- [10] A. Di Piazza, C. Müller, K. Z. Hatsagortsyan, C. H. Keitel, *Rev. Mod. Phys.* **84**, 1177 (2012).
- [11] D. A. Burton, A. Noble, *Contemp. Phys.* **55**, 110 (2014).
- [12] W. Dittrich, M. Reuter, *Effective Lagrangians in Quantum Electrodynamics* (Springer, Heidelberg, 1985).
- [13] E. S. Fradkin, D. M. Gitman, Sh. M. Shvartsman, *Quantum Electrodynamics with Unstable Vacuum* (Springer, Berlin, 1991).
- [14] V. N. Baier, V. M. Katkov, V. M. Strakhovenko, *Electromagnetic Processes at High Energies in Oriented Single Crystals* (World Scientific, Singapore, 1998).
- [15] A. Di Piazza, K. Z. Hatsagortsyan, C. H. Keitel, *Phys. Rev. Lett.* **105**, 220403 (2010).
- [16] T. G. Blackburn, C. P. Ridgers, J. G. Kirk, A. R. Bell, *Phys. Rev. Lett.* **112**, 015001 (2014).
- [17] N. Neitz, A. Di Piazza, *Phys. Rev. Lett.* **111**, 054802 (2013).
- [18] V. Ritus, *Journal of Soviet Laser Research* **6**, 497 (1985).

- [19] Y. Kravets, A. Noble, D. Jaroszynski, *Phys. Rev. E* **88**, 011201 (2013).
- [20] N. Kumar, K. Z. Hatsagortsyan, C. H. Keitel, *Phys. Rev. Lett.* **111**, 105001 (2013).
- [21] A. V. Bashinov, A. V. Kim, *Phys. Plasmas* **20**, 113111 (2013).
- [22] A. Ilderton, G. Torgrimsson, *Phys. Lett. B* **725**, 481 (2013).
- [23] L. L. Ji, A. Pukhov, I. Y. Kostyukov, B. F. Shen, K. Akli, *Phys. Rev. Lett.* **112**, 145003 (2014).
- [24] J.-X. Li, K. Z. Hatsagortsyan, C. H. Keitel, *Phys. Rev. Lett.* **113**, 044801 (2014).
- [25] R. Capdessus, P. McKenna, *Phys. Rev. E* **91**, 053105 (2015).
- [26] M. Vranic, T. Grismayer, R. A. Fonseca, L. O. Silva, *New J. Phys.* **18**, 073035 (2016).
- [27] V. Dinu, C. Harvey, A. Ilderton, M. Marklund, G. Torgrimsson, *Phys. Rev. Lett.* **116**, 044801 (2016).
- [28] A. Di Piazza, T. N. Wistisen, U. I. Uggerhøj, *Phys. Lett. B* **765**, 1 (2017).
- [29] R. Medenwaldt, *et al.*, *Phys. Rev. Lett.* **63**, 2827 (1989).
- [30] J. Beringer, *et al.*, *Phys. Rev. D* **86**, 010001 (2012).
- [31] L. D. Landau, E. M. Lifshitz, *The Classical Theory of Fields* (Elsevier, Oxford, 1975).
- [32] J. D. Jackson, *Classical Electrodynamics* (Wiley, New York, 1975).
- [33] S. P. Møller, *Nucl. Instrum. Methods Phys. Res. A* **361**, 403 (1995).
- [34] I. V. Sokolov, J. A. Nees, V. P. Yanovsky, N. M. Naumova, G. A. Mourou, *Phys. Rev. E* **81**, 036412 (2010).

- [35] N. Neitz, A. Di Piazza, *Phys. Rev. Lett.* **111**, 054802 (2013).
- [36] V. N. Baier, V. M. Katkov, V. M. Strakhovenko, *Electromagnetic Processes at High Energies in Oriented Single Crystals* (World Scientific, Singapore, 1998).
- [37] K. Yokoya, *SLAC KEK-Report-85-9* (1985).
- [38] T. G. Blackburn, C. P. Ridgers, J. G. Kirk, A. R. Bell, *Phys. Rev. Lett.* **112**, 015001 (2014).
- [39] A. Di Piazza, K. Z. Hatsagortsyan, C. H. Keitel, *Phys. Rev. Lett.* **105**, 220403 (2010).
- [40] A. Belkacem, N. Cue, J. Kimball, *Phys. Lett. A* **111**, 86 (1985).
- [41] T. N. Wistisen, *Phys. Rev. D* **90**, 125008 (2014).
- [42] T. N. Wistisen, *Phys. Rev. D* **92**, 045045 (2015).
- [43] L. Bandiera, E. Bagli, V. Guidi, V. V. Tikhomirov, *Nucl. Instr. Methods Phys. Res. B* **355**, 44 (2015).
- [44] V. Guidi, L. Bandiera, V. V. Tikhomirov, *Phys. Rev. A* **86**, 042903 (2012).
- [45] J. Beringer, *et al.*, *Phys. Rev. D* **86**, 010001 (2012).

Acknowledgments

We acknowledge the technical help and expertise from Per Bluhme Christensen, Erik Loft Larsen and Frank Dagaard (AU) in setting up the experiment and data acquisition.

Authors' contribution

TNW and UIU conceived and carried out the experiment. TNW and ADP carried out the theoretical calculations. TNW carried out the data analysis. TNW and ADP wrote the paper with input and discussion from HVK and UIU.